BIOMIMETIC POLYSACCHARIDE/BIOACTIVE GLASS NANOPARTICLES MULTILAYER MEMBRANES FOR GUIDED TISSUE REGENERATION

José R. Rodrigues[1,2], Natália M. Alves[1,2]*, João F. Mano[1,2]*#.

[1] 3B's Research Group, Biomaterials, Biodegradables and Biomimetics, University of Minho, Headquarters of the European Institute of Excellence on Tissue Engineering and Regenerative Medicine, AvePark-Parque de Ciência e Tecnologia, 4805-017 Barco, Guimarães, Portugal
[2] ICVS/3B's, Associate PT Government Laboratory, Braga/Guimarães, Portugal
* Authors for correspondence: nalves@dep.uminho.pt; jmano@ua.pt
# Current address: Department of Chemistry, CICECO – Aveiro Institute of Materials, University of Aveiro, 3810-193 Aveiro, Portugal

Abstract

Nowadays, guided tissue regeneration (GTR) research is centred in the development of composite bioabsorbable membranes with enhanced bioactivity and with processing controlled at the nanoscale. Inspired by this new focus of GTR research and also by nacre structure, layered freestanding membranes were produced using the Layer-by-Layer (LbL) deposition technique, combining chitosan (CHI), hyaluronic acid (HA) and bioactive glass nanoparticles (BGNPs). It is expected that the combination of these materials processed by this particular technique will result in nanostructured membranes with enhanced mechanical performance as well as improved bioactivity. Moreover, the effect of the modification of HA with catechol groups (HAD) on the adhesive properties of the membranes was also analysed. The results showed that it was possible to produce biomimetic membranes with different surface properties, improved adhesive strength and the ability to induce the formation of apatite, necessary for the formation of new bone. It was also possible to control the BGNPs content of the membranes by use of HAD instead of unmodified HA and changing the number of BGNPs' deposition steps. Moreover, it was shown that membranes with different concentrations of BGNPs possess different mechanical performance, swelling properties and degradation behaviour, which indicates the possibility to tune the membranes' properties by controlling the deposition of BGNPs onto the membranes.

Keywords: Guided Tissue Regeneration; Tissue Engineering; Layer-by-Layer; Nanocomposites; Structural Biomaterials;

1. INTRODUCTION

One of the main challenges in periodontal regeneration comes from the different migration rates that its different cellular components possess. This could lead to invasion of gingival fibroblasts into mandibular bone defects and compromise proper bone regeneration (1-3). Guided Tissue Regeneration (GTR) aims to prevent fibroblast invasion and to allow new bone formation by using a membrane that acts as a barrier to invading cells and as a scaffold for bone regeneration (3, 4).

The ideal GTR membrane should exhibit biocompatibility with the host tissues, a proper degradation profile, and adequate mechanical and physical properties to allow its implementation *in vivo* and sufficient sustained strength to avoid membrane collapse (2). However, the currently available membranes do not show all of these characteristics. At the present day, the gold standard GTR membranes are made of non-resorbable materials such as dense polytetrafluoroethylene (d-PTFE), which need to be surgically removed after treatment, leading to additional pain and discomfort to the patient and higher economic costs (3, 4).

Some resorbable GTR membranes, both from synthetic and natural origins, are already commercially available. Most of the resorbable GTR membranes based on synthetic materials are produced using polyesters, namely poly (glycolic acid), poly (lactic acid), poly (ε-caprolactone) and their copolymers. Membranes produced with these polymers are biocompatible, biodegradable and easier to handle clinically when compared to the existing non-resorbable membranes, and allow tissue integration. However, while polyester based membranes initially possess adequate mechanical properties to be functional, after 4 weeks on incubation in culture medium, these membranes completely lose their structural and mechanical properties and, hence, their functionality. As for natural-based GTR membranes, the available ones are generally produced with collagen, which not only offer excellent cell affinity and biocompatibility, as it is also a major constituent of the extracellular matrix (ECM). Nevertheless, these membranes also present drawbacks, as they have been shown to have poor mechanical strength and performance *in vivo*, unpredictable degradation and, due to their human or animal origin, increased risk of transmitting diseases (3, 4).

To eliminate the need of a second surgery and to prevent the premature failure of the treatment, current GTR research is focused on the development of bioabsorbable membranes which must not only possess adequate mechanical properties, but should also maintain their functionality for 4 to 6 weeks. As to further improve their properties, the new membranes should also present bioactivity and there are advantages if their production method should be controlled down to the nanoscale (3, 4).

Due to its outstanding mechanical properties, there has been an increased interest in producing new materials mimicking nacre (5). Nacre, a component of the shell of most molluscs of the bivalve and gastropod classes, is a natural composite consisting in a hierarchical layered structure that combines aragonite (a crystallographic form of $CaCO_3$) and an organic matrix (6, 7). This combination of layered organic and inorganic components results in a material that has both increased mechanical resistance and toughness, when compared to pure organic and inorganic materials, respectively (4, 6-9). Several techniques have been developed to produce nacre-like structures, being Layer-by-Layer (LbL) a particularly interesting option due to its ability to process several different materials and to control the thickness of the produced structure at the nanoscale level (10-12).

The LbL deposition technique is normally achieved by exploring electrostatic interactions, with the alternate immersion of the substrate in opposite charged polyelectrolyte solutions (11-13). LbL structures have also been produced by exploring hydrogen and covalent bonding, charge transfer, biologic recognition and hydrophobic interactions (14). As such, many different materials can used in LbL, including polyelectrolyte solutions, biological polysaccharides, nanoparticles, among others (11, 15). Depending on the used substrate, several different structures can be obtained by the LbL deposition, including freestanding membranes (11, 16). These membranes can, for example, be easily obtained by using substrates with low surface energy without the use of additional sacrificial layers (17-19).

Inspired by the new focus of GTR research, this work proposes the development of nacre-like layered freestanding membranes using the LbL technique. The organic phase will be composed by natural polymers such as chitosan (CHI) and hyaluronic acid (HA). Both these materials have already successfully been used to produce LbL coatings and freestanding structures (17, 20, 21). HA will also be modified with dopamine containing catechol groups, as to improve the membranes adhesive properties (21-23). This modification of HA (HAD) is based on the adhesive properties present in

mussels' adhesive proteins (MAPs). Such properties have been attributed mainly to the amino-acid 3, 4-dihydroxy-L-phenylalanine (DOPA) and the catechol groups present in this amino-acid, which are responsible for the strong bonds established between mussels and different structures, even in wet conditions (23-25).

The inorganic phase will be composed of ternary bioactive glass nanoparticles (BGNPs) produced by a sol-gel method, which are able to induce the precipitation of hydroxyapatite at their surface (26, 27). It expected that the inclusion of these BGNPs will not only improve the mechanical properties of the produced membranes, but will also confer a bioactive character to the membranes.

2. MATERIALS AND METHODS

2.1 Materials

HA sodium salt from *Streptococcus equi* (Mw=1.5-1.8 $\times 10^6$ Da), dopamine hydrochloride (Mw=189.64 Da), N-(3-Dimethylaminopropyl)-N′-ethylcarbodiimide hydrochloride (EDC) (Mw=191.70 Da), citric acid monohydrate (purity > 99.0%, Mw=210.14 Da), ammonium phosphate dibasic (purity > 98.0%, Mw=132.06 Da), calcium nitrate tetrahydrate (purity > 99.0%, Mw=236.15 Da), ethanol absolute, ammonium hydroxide solution (30-33% in water, D=0.9 $g.ml^{-1}$ at 25 °C), CHI of medium molecular weight (degree of N-deacetylation = 75-85%, μ= of 200-800 cP), sodium chloride, sodium hydrogen carbonate, potassium chloride, di-sodium hydrogen phosphate trihydrate, magnesium chloride hexahydrate ($MgCl_2 \cdot 6H_2O$), calcium chloride, sodium sulfate, Tris(hydroxymethyl)-aminomethan (Tris buffer) and hydrochloric acid were all purchased from Sigma-Aldrich (Germany). Before its use, CHI was purified via a recrystallization process. In acidic medium, HA is a negatively charged polyelectrolyte (pKa≈2.9) and CHI is a positively charged polyelectrolyte (pKa≈6.5). Tetraethyl orthosilicate (TEOS) (purity = 99.0%, Mw=208.33 Da) and glutaraldehyde 25% (wt.) aqueous solution (purity >= 98%, Mw=100.1 Da) were purchase from Merck Chemicals (Germany). Before its use, the glutaraldehyde solution was diluted to 1% (wt.) using ultrapure water.

2.2 Methods

2.2.1 Synthesis of the Hyaluronic Acid-Dopamine Conjugate

Hyaluronic acid (HA) was chemically modified with catechol groups to form a hyaluronic acid-dopamine (HAD) conjugate. HAD was produced using 1-ethyl-3-(3-dimethylaminopropyl) carbodiimide hydrochloride (EDC), a zero-length activation agent used to bound carboxyl groups to primary amines. The process for HA modification used was first proposed by Lee *et al*. (23).

The first step involves the dissolution of 1g of HA in 100 mL of phosphate buffered saline solution (PBS), followed by adjusting the pH to 5.5 with solutions of 0.5M hydrochloric acid (HCl) or 0.5M sodium hydroxide (NaOH) solution. The solution was then purged with nitrogen for 30 minutes to limit oxygen interaction, since dopamine is air sensitive and the solution becomes darker when a reaction with oxygen occurs. Afterwards, 338 mg of EDC and 474 mg of dopamine were added to the previous solution, and left to react for 2 h. The last step consists of a week-long removal through dialysis of all unreacted chemicals and urea bi-products, followed by lyophilisation for 4 days.

The produced HAD conjugate is not only sensitive to air, but also to light and temperature. As such, all reactions were performed at 4 ºC and protected from light, as to avoid dopamine oxidation. The conjugate was also stored at 4 ºC and protected from light.

2.2.2 Production of the Ternary Bioactive Glass Nanoparticles

Ternary Bioactive Glass Nanoparticles (BGNPs) were prepared based on a previously proposed protocol, in which BGNPs were produced with a SiO_2:CaO:P_2O_5 (mol.%)= 50:45:5 system, using an optimized sol-gel method (26, 27).

Production of the BGNPs involves a series of sequential reagent dissolutions resulting in hydrolysis and polycondensation reactions. First, 7.639 g of Calcium Nitrate were dissolved in 120 ml of deionized water at room temperature. Calcium Nitrate was used as the Ca precursor. After that, 9.8353 ml of tetraethyl orthosilicate (TEOS), used as the Si precursor, were added with 60 ml of ethanol to the previous solution. The pH was adjusted to 2 with 30 ml of a citric acid solution (10%), to promote hydrolysis, and the reaction was left under stirring during 3 hours, resulting in solution A. To prepare solution B, 1.078g of $(NH_4)_2HPO_4$, used as P precursor, were added to 1500 ml of deionized water, and the pH was adjusted to 11.5 with an ammonium hydroxide solution. Both ethanol and ammonia were used as the jellifying agents.

After both solutions were prepared, the solution A was added drop-by-drop to the solution B, under stirring. At the same time, the pH of solution B was maintained at 11.5 by adding an ammonium hydroxide solution B. The obtained mixture was left under stirring for 48 hours. The resulting precipitate was then washed 3 times using 500 ml of deionized water.

The obtained gel slurry was stored for at least 24 hours at -80 ºC, followed by freeze-drying for 7 days. The obtained white gel powder was then calcinated at 700 ºC for 5 hours. This step allows to not only obtain the BGNPs, but also improves the particles bioactivity and removes the remaining ammonium.

2.2.3 Production of the Freestanding Membranes using Layer-by-Layer

Four different polyelectrolyte (PE) solutions were prepared, containing CHI, HA, HAD and BGNPs, respectively. The concentration of each PE is present in Table 1. All PE solutions were prepared in a 0.15 M solution of NaCl. For the CHI solution it was added 1% (v/v) of acetic acid to the NaCl solution, as CHI is only soluble in acidic conditions. The PE solutions were prepared under stirring and left dissolving overnight. The pH of the PE solutions was adjusted to 5.5 using solutions of NaOH (2 M for the CHI solution, 1 M for the remaining PE) and one of 1% (v/v) of acetic acid. A 0.15 M solution of NaCl, with the pH adjusted to 5.5, was used as the washing solution.

Three different procedures were used to produce four different types of membranes, as shown in Table 1. Regardless of the chosen procedure, all membranes were produced with 300 layers.

Table 1 – Procedures for the formation of the freestanding LbL membranes

Procedure	Formulation	PE concentration
1	**1:** $(CHI\text{-}HA)_{150}$	CHI: 2.0 mg/ml HA: 2.0 mg/ml
2	**2:** $(CHI\text{-}HA\text{-}CHI\text{-}BGNPs)_{75}$	CHI: 2.0 mg/ml HA: 2.0 mg/ml BGNPs: 2.5 mg/ml
2	**3:** $(CHI\text{-}HAD\text{-}CHI\text{-}BGNPs)_{75}$	CHI: 2.0 mg/ml HAD: 2.0 mg/ml BGNPs: 2.5 mg/ml
3	**4:** $(1)_{37}\text{-}(2)_{38}\text{-}(1)_{37}$	CHI: 2.0 mg/ml HA: 2.0 mg/ml

BGNPs: 2.5 mg/ml

Procedure 1 was used to produce the control membranes, composed by CHI and HA (formulation 1). After each cycle – see Figure 1 A – one CHI-HA bi-layer is produced. The dip coating equipment was programmed to run for 150 cycles.

Procedure 2 was used to produce membranes with the formulations 2 and 3. After each cycle – see Figure 1 B – two bi-layers are produced, the first composed of CHI-HA or CHI-HAD and the second composed of CHI-BGNPs. To avoid the particle aggregation, the solutions containing BGNPs were kept under stirring and periodically subjected to an ultrasonic treatment.

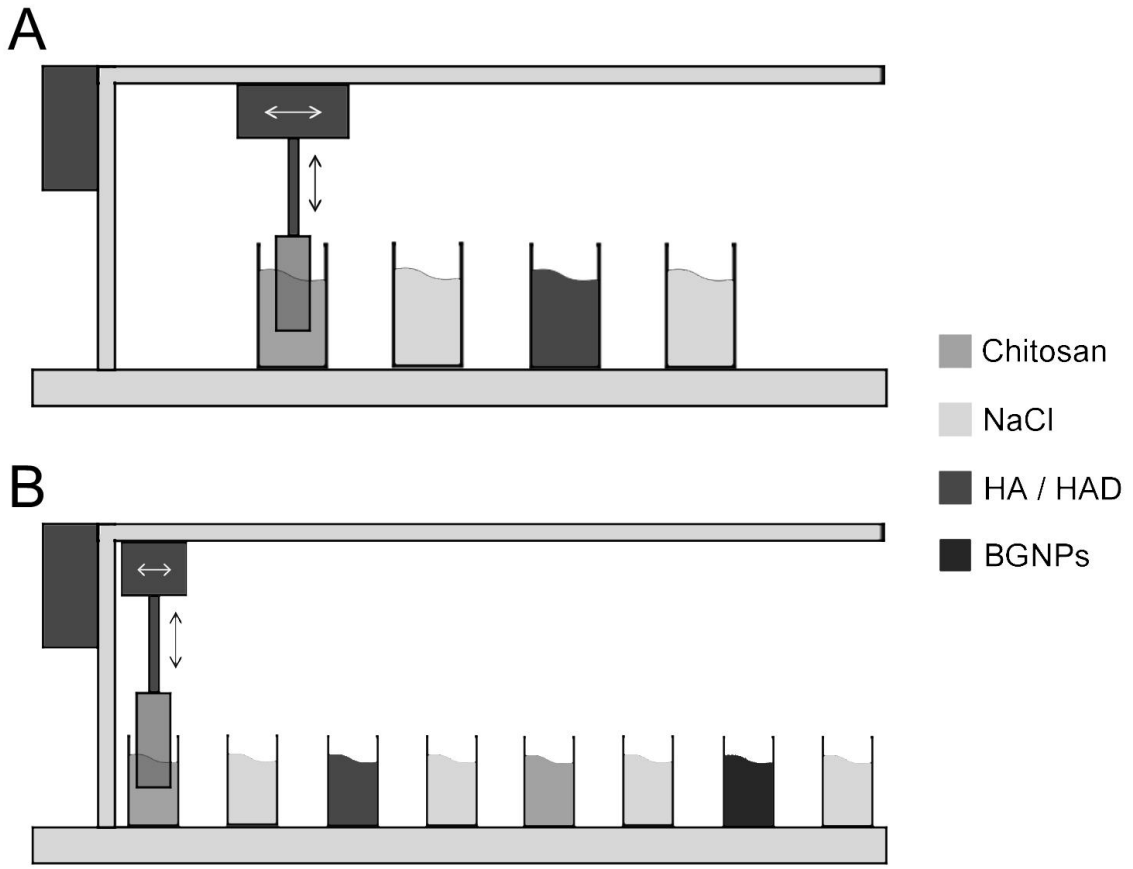

Figure 1 – Schematics representing one cycle of (A) procedure 1 and (B) procedure 2.

Procedure 3 was used to produce membranes following the formulation 4. This is a combination of procedures 1 and 2. First, 37 cycles of procedure 1 were run to produce 37 bi-layers composed of CHI-HA. Then, 38 cycles of procedure 2 were run to produce 76 bi-layers, alternating CHI-HA bi-layers with CHI-BGNP bi-layers. Finally, 37 cycles of procedure 1 were again run as to produce 37 bi-layers composed of CHI-

HA. The resulting membranes were composed by external bi-layers consisting of CHI-HA and internal bi-layers composed by CHI-HA intercalated with CHI-BGNP.

In all procedures, dipping times were of 10 min for the CHI, HA and HAD solutions, 20 min for the BGNPs suspension and 5 min for the washing solution.

At the end of each procedure, the substrates were left to dry for 4 days in 100 ml cups covered with punctured aluminium foil. The membranes were then removed from the substrates with the help of a tweezer.

To further improve the stability and mechanical performance of the freestanding LbL membranes, they were crosslinked following a protocol based on the one proposed by Larkin *et al.* (17). The membranes were soaked in a 1% (wt.) solution of glutaraldehyde for 1 minute, following by 3 washing-steps in distilled water. This allows to remove the crosslinking agent that didn't react and any salt deposition derived from the LbL deposition process. The membranes were then left to dry at room temperature, overnight. To prevent membrane shrinkage and ripple, the membranes were covered with glass slides.

2.2.4 Thermogravimetric Analysis

TGA measurements were performed to quantify the amount of BGNPs present in the freestanding LbL membranes. It was used a Q500 TGA equipment (TA Instruments, USA). The mass variation was monitored between 40 °C and 800 °C at a heating rate of 10 °C/min. The amount of BGNPs present in each formulation was calculated following Equation (1):

$$B\ (\%) = \frac{R_f - R}{100 - R} \times 100 \quad (1)$$

where B is the amount of BGNPs (%), R the residual weight of the control membranes (formulation 1) and R_f the residual weight of the BGNPs-containing membrane.

2.2.5 Surface Characterization

The morphology of both surfaces of the freestanding membranes was characterized by scanning electron morphology (SEM), using a JSM-6010LV SEM-EDS (JEOL, Japan).

The wettability of the freestanding LbL membranes was assessed by water contact angle (WCA) measurement using an OCA15plus goniometer equipment (DataPhysics, Germany). For each surface of each membrane, 10 measurements were made, using 1 µl droplets of distilled water dispensed by a motor-driven syringe. The measurements were performed at room temperature and the pictures taken immediately after the drop contact the surface. The results' treatment was performed using the SCA20 software.

2.2.6 Water Uptake

For the produced freestanding LbL membranes, WU was measured by soaking previously weighed dry membranes in a phosphate buffer saline (PBS) solution for specific time periods. The swollen membranes were removed and carefully dried after each time point. The dried samples were weighed with an analytical balance. WU was measured following Equation (2):

$$WU(\%) = \frac{W_w - W_d}{W_d} \times 100 \quad (2)$$

where W_w is the weight of the swollen membranes and W_d is the weight in dry conditions. Each experiment was repeated three times and the average value was taken as the WU.

2.2.7 Weight Loss

To evaluate the weight loss (WL) of the freestanding LbL membranes, previously weighed samples were soaked in a PBS solution for 1, 7, 14 and 21 days, at 37ºC. The membranes were removed from the PBS solution, carefully washed and dried at each time point. The dried samples were weighed with an analytical balance. WL was calculated following Equation (3):

$$WL(\%) = \frac{W_i - W_f}{W_i} \times 100 \quad (3)$$

where W_i is the initial dry weight of the sample and W_f its final dry weight after each time point. Each experiment was repeated three times and the average value was taken as the WL.

2.2.8 Mechanical Characterization

Tensile strength and adhesive strength tests were performed using a universal mechanical testing (UMT) equipment (Instron 5543, USA), equipped with a 1 kN load cell.

For tensile strength tests, the specimens were cut in rectangular shapes (30 mm length and 5 mm width) and soaked in a PBS solution overnight. Measurements were taken under a load speed of 1 mm/min and a gauge length of 10 mm. Three samples were tested for each composition in order to calculate the mean and standard deviation value of Elastic modulus, ultimate tensile strength and strain at failure.

For the adhesive strength tests, the specimens were cut in rectangular shapes (35 mm length and 10 mm width), cut in half and place in contact in order to have a contact area of 5 mm length and 10 mm width. The membranes were soaked with distilled water and pressure was applied for 1 minute. Water excess was removed using filter paper and the membranes dried at room temperature overnight. Measurements were taken under a loading speed of 0.5 mm/min and a gauge length of 10 mm. Three samples were tested for each composition in order to calculate the mean and standard deviation value of the ultimate adhesion strength.

2.2.9 In vitro bioactivity tests

In vitro bioactivity was assessed by immersing samples of each membrane in simulated body fluid (SBF) at 37 °C for 7 days. After 7 days, the samples were carefully washed in distilled water and dried at room temperature for 24 hours. SBF was produced following the protocol developed by Kokubo and Takadama (28). To evaluate the formation of apatite we used SEM, energy dispersive X-ray spectroscopy (EDS) and Fourier transform infrared (FTIR). SEM and EDS were conducted with a JSM-6010LV SEM-EDS (JEOL, Japan). FTIR analysis was conducted with a Spotlight 300 FTIR microscope with spectrum 100 FTIR spectrometer (Perkin-Elmer, USA). The spectra were obtained under the wave number range of 1300-400 cm^{-1}.

3. RESULTS AND DISCUSSION

3.1 Production of the Freestanding Membranes using Layer-by-Layer

Photographs of the macroscopic morphology of the produced LbL membranes are shown in Figure 2. It can be observed that it was possible to produce thin membranes following all 4 planned formulations. It is also possible to observe that the membranes with formulations 1 and 4 are transparent, while the membranes with formulations 2 and 3 are opaque. This is due to the higher BGNPs concentration present in formulations 2 and 3, which seems to be sufficient to alter the optical properties of the membranes. Formulation 4, which has fewer BGNPs deposition steps, retains the transparent look found in formulation 1, which does not contain BGNPs. It was also found that the higher BGNPs concentration present in formulations 2 and 3 also turn the membranes stiffer, even before crosslinking with glutaraldehyde, while formulations 1 and 4 have a flexible behaviour, before crosslinking. Quantitative mechanical results will be shown later.

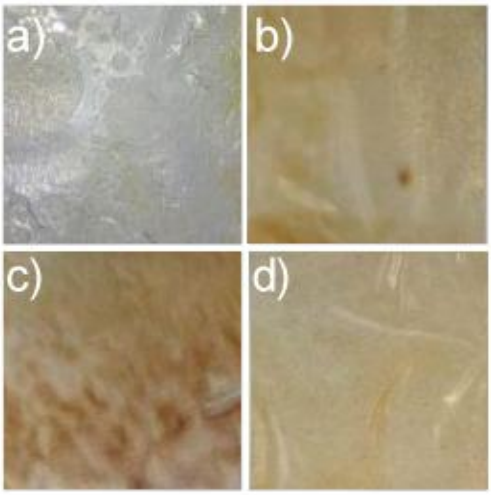

Figure 2 – Photographs of the macroscopic morphology of the produced membranes, after crosslinking with 1% (wt.) glutaraldehyde: a) Formulation 1; b) Formulation 2; c) Formulation 3; d) Formulation 4.

The yellow coloration observed in the membranes comes from the crosslinking with glutaraldehyde. The effect of the crosslinking also altered the mechanical properties of the membranes, as formulations 1 and 4, which were flexible before crosslinking, became stiffer. This step was necessary as freestanding membranes produced with CHI and HA that were not subjected to a crosslinking agent are not stable when immersed in water (17, 29). Glutaraldehyde, which allows for the covalent bonding of the amine groups present in CHI and HA (30), was found to stabilize the structure of the resulting films (17, 29). The exposure of the membranes to a 1% (wt.)

solution of glutaraldehyde for 1 minute was sufficient to overcome their instability in wet conditions.

3.2 Thermogravimetric Analysis

TGA analysis was conducted to quantify the relative quantity of BGNPs present in each membrane formulation. Figure 3 shows the obtained results, where three different slopes could be identified: the first, until 100 °C, represents the evaporation of residual humidity that the membranes may possess. The small weight gain detected in formulation 3 between this range of temperatures may be due to the decrease in gas density, which could push the hanged sample down and be detected as weight gain (31). The second one, which goes between 200 °C to 400 °C, represents the loss of organic matter, namely CHI, HA and HAD. The final one may come from the loss of the residual ashes. In the end, the weight residue for formulation 1 was of 22.5%, 56.7% for formulation 2, 65.9% for formulation 3, and 34.9% for formulation 4. These different values come from the presence of BGNPs in formulations 2, 3 and 4, which further indicates the successful deposition of these particles into the freestanding membranes.

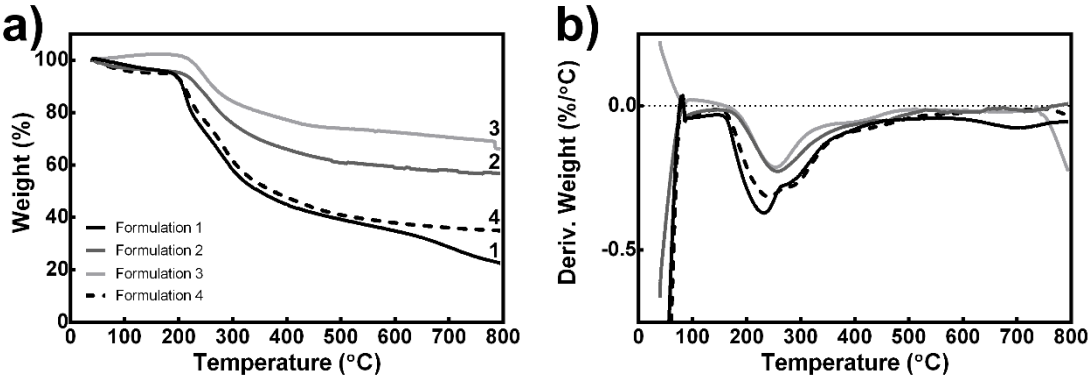

Figure 3 – Thermogravimetric analysis representation: a) TGA curves for the produced freestanding LbL membranes. Final weight loss was of 22.5% for formulation 1; 56.7% for formulation 2; 65.9% for formulation 3; 34.9% for formulation 4; b) Derivate of the weight curves as function of temperature (°C).

The results also show that these membranes do not possess the same BGNPs quantity, when compared to each other. When applying Equation (1), it can be estimated that BGNPs represent 44.12% of the composition of formulation 2, 56.0% of formulation 3 and 16.0% of formulation 4. These values are according to what was expected. Formulation 4 has fewer BGNPs deposition steps, which results in the deposition of a lower quantity of BGNPs onto the freestanding membranes. Formulation 3 has an overall higher BGNPs quantity on its composition, when compared to formulation 2. This feature could be explained by the catechol groups present in the

HAD conjugate, which are able to create a strong bond with several materials, including glass (32-34). As such, it can be speculated that, in formulation 3, BGNPs deposition onto the freestanding membranes comes not only from charged interactions between the surface of the membrane and the BGNPs, but also due to the bounding of BGNPs with the catechol groups present in the HAD conjugate. Both these mechanisms, acting simultaneously during the production of freestanding LbL membranes, may be able to induce the deposition of a higher concentration of BGNPs onto the membranes.

3.3 Surface Characterization

The morphology of the produced membranes was analysed by SEM – see Figure 4. For analysis purposes, "upper surface" refers to the first layer produced, facing the substrate and composed by CHI, while "down surface" refers to the last layer produced, composed of HA in formulations 1 and 4 and BGNPs in formulations 2 and 3.

There are some slight differences in the morphology between the surfaces of all membranes. The surfaces from formulations 2 and 3 seem to have a rougher morphology, compared to the smoother surfaces present in formulations 1 and 4. Such difference of roughness should be a consequence of the BGNPs in the surface of formulations 2 and 3, and could have implications in several properties, including cell behaviour (11, 35).

To further study the properties of both surfaces of the produced membranes, their wettability was also assessed by WCA – see Figure 5.

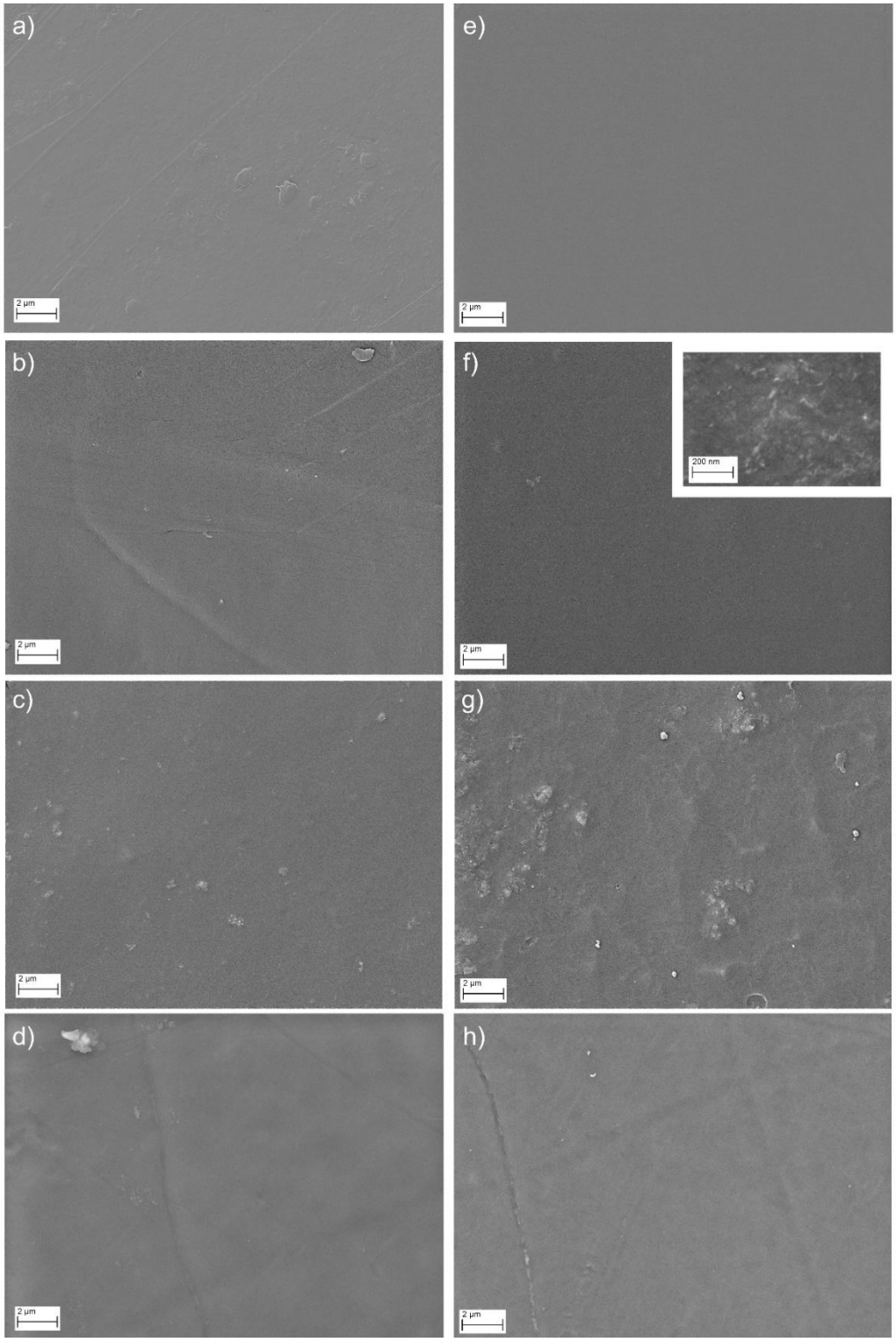

Figure 4 – SEM images of the produced freestanding membranes: a) formulation 1, upper surface; b) formulation 2, upper surface; c) formulation 3, upper surface; d) formulation 4, upper surface; e) formulation 1, down surface; f) formulation 2, down surface; g) formulation 3, down surface; h) formulation 4, down surface.

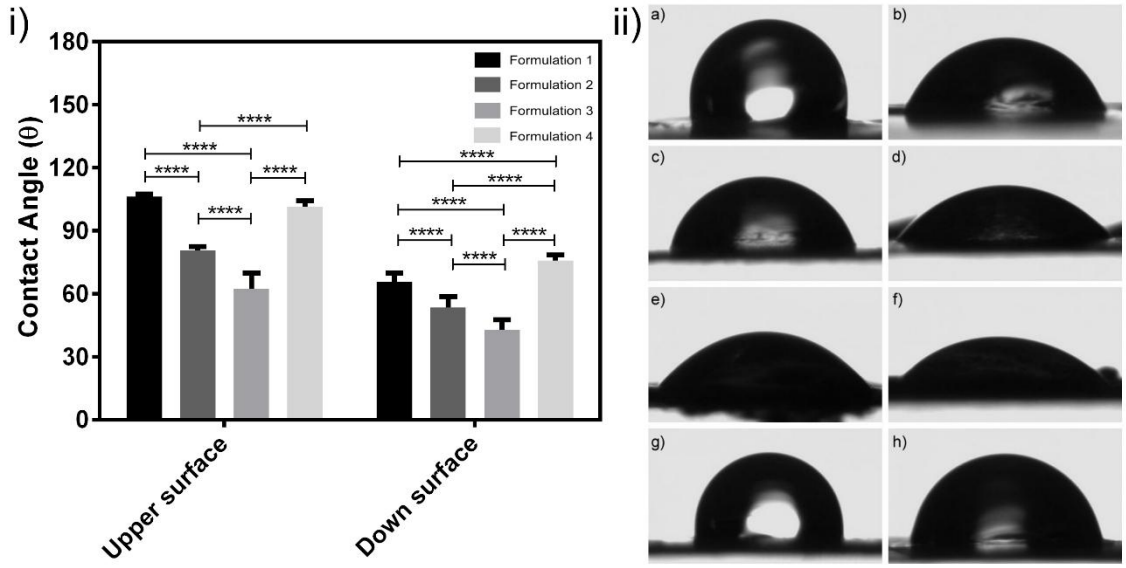

Figure 5 – i: Water contact angles measured for each surface of each membrane. Data are means + standard deviation (n = 10, **** significantly different [two-way ANOVA, $p < 0.0001$]); **ii:** Example of water drops for each surface of each membrane: a) formulation 1, upper surface; b) formulation 1, down surface; c) formulation 2, upper surface; d) formulation 2, down surface; e) formulation 3, upper surface; f) formulation 3, down surface; g) formulation 4, upper surface; h) formulation 4, down surface.

The down surface of all membranes present a more hydrophilic behaviour when compared to the upper surface. This difference in wettability could be used to produce membranes with asymmetrical biologic response. This could be especially relevant in GTR applications, as the two surfaces of the membrane will face the gingival epithelium or the alveolar bone defect. In theory, this could lead to an improved bone regeneration, while diminishing the risk of invasion of epithelium cells to the defect (1, 3, 4, 35).

The presence of BGNPs also seems to deeply affect the wettability of the membranes, regardless of the analysed surface. In fact, the presence of a higher content of BGNPs in formulations 2 and 3 is capable of turning their upper surface hydrophilic, compared to the hydrophobicity of the upper surface observed in formulations 1 and 4. The presence of a higher content in BGNPs had also an effect on the wettability of the down surfaces, as the measured WCA in formulations 2 and 3 were significantly lower than those measured in formulations 1 and 4. These results are expected as the presence of BG particles at the surface of a composite is able to increase its hydrophilicity (36, 37). Hydrophilicity is also affected by BGNPs concentration, as shown by the significantly lower contact angles corresponding to the surfaces of formulation 3, when compared with formulation 2.

3.4 Water Uptake

The WU of the distinct membranes was evaluated for 24 hours in PBS at 37 °C – see Figure 6 a). For the membranes following the formulation 1, composed of CHI and HA, the swelling equilibrium was reached after 1 hour, with a WU of approximately 340%. For the other membranes, the behaviour depends on the formulation. Formulation 2 shows a substantial decrease in WU that can be derived from its high BGNPs content, which results in a lower polymeric content, and thus to a decrease in WU. However, formulation 3, which possesses an even higher BGNPs content (and consequent lower polymeric content) has a WU of a similar magnitude than the one reached by formulation 1. However, as shown in Figure 4, the membranes with formulation 3 are significantly more hydrophilic than the membranes with formulation 2. This significant higher affinity to water could explain the increased WU in formulation 3, when compared with formulation 2.

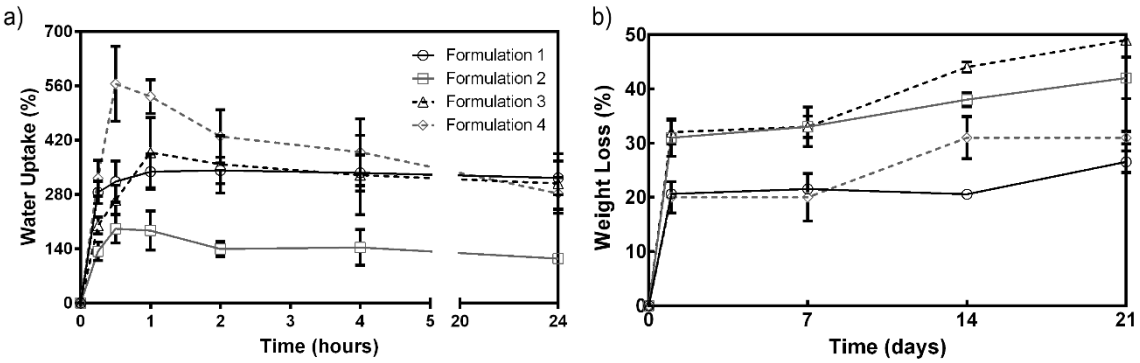

Figure 6 – a) Water uptake for the freestanding Layer-by-Layer membranes; b) Weight loss for the freestanding membranes.

Membranes with formulation 4 seem to have a high initial WU, when compared to all other formulations, which is followed by a quick decrease in WU to values of the same magnitude as the ones achieved by formulations 1 and 3. This can be due to an increased osmotic pressure into the membrane due to the presence of BGNPs only in its interior. The equilibrium of osmotic pressures inside and outside the membrane may then explain the decrease in WU shown by these membranes. The decrease in WU may also be explained by a quicker release of the BGNPs from the membranes' interior, as an increase in WU can lead to an increase of WL (38, 39).

The quick decrease in WU is not only observed in formulation 4, as formulations 2 and 3 also show a decrease in WU, albeit in a smaller scale, which is followed by a stabilisation of their swelling ability. In all cases, this decrease in WU may be explained by the release of BGNPs from the membranes – see next section.

3.5 Weight Loss

The study of the degradation profile of membranes for GTR is of great importance, as they should be able to preserve their structural and mechanical integrity for 4 to 6 weeks (3, 4). Figure 6 b) shows the degradation profile for the produced membranes in PBS solution at 37 °C, for a period of 21 days.

After 1 day, there is a substantial difference in WL between formulations 1 and 4 (approximately 20%), compared to formulations 2 and 3 (approximately 33%). This may come from the release of BGNPs from membranes with formulations 2 and 3, richer in inorganic content, which can lead to an increase of membrane WL. As the membranes with formulation 4 only possess BGNPs in their interior, their degradation profile is initially similar to that of formulation 1. However, after 14 days, there is an increase in WL in formulation 4, which may be related to the degradation of their external layers, which potentiates the release of BGNPs from its interior.

Regarding formulations 2 and 3, their degradation profiles are also similar until day 14, where the WL for formulation 3 starts to get higher. Two factors may explain the increase in WL for formulation 3. First, the higher BGNPs content in formulation 3, which may lead to an increased BGNPs release and, therefore, to an increase in WL. Also, as formulation 3 has a higher WU than formulation 2, this can also lead to the higher WL levels found in formulation 3 (38, 39). The dissolution of the BGNPs component may be relevant for the bioactivity of the membranes, which will be investigated later.

3.6 Mechanical Characterization

To assess the mechanical properties of the produced freestanding membranes, tensile strength assays were performed to determine the membranes' Elastic modulus (E), ultimate tensile strength (σ) and length at break (ε) - see Figure 7.

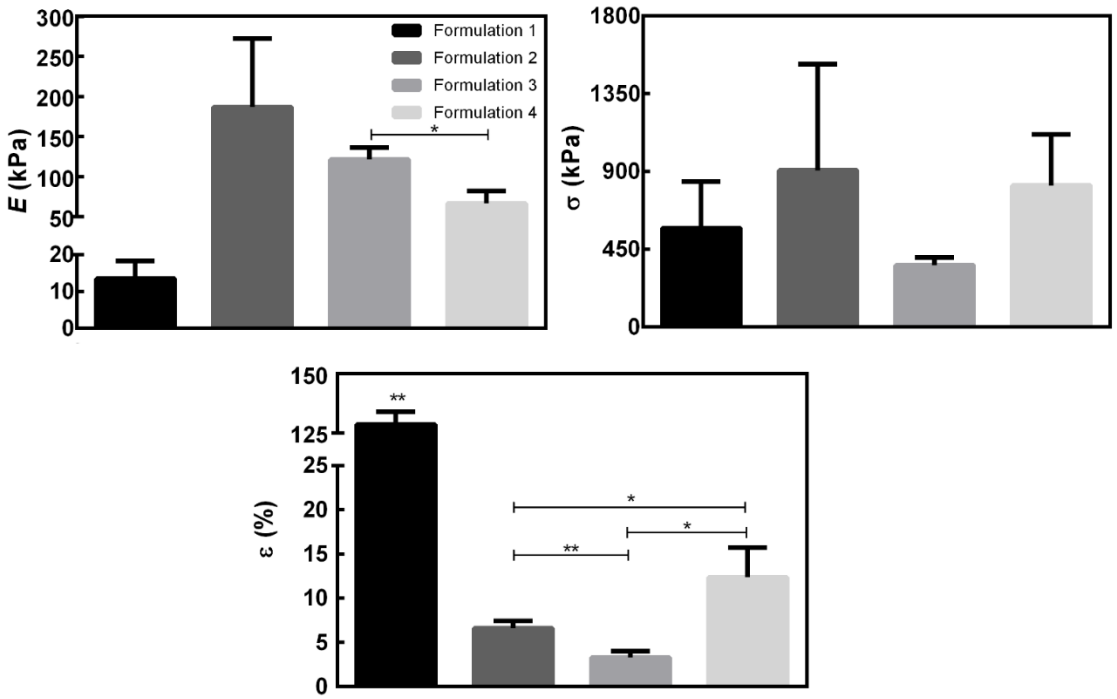

Figure 7 –. Elastic modulus (*E*), ultimate tensile strength (σ) and length at break (ε) for the freestanding Layer-by-Layer membranes. Data are means + standard deviation (n = 3, * significantly different [t-Student test, $p<0.05$]; ** significantly different [t-Student test, $p<0.01$]).

Formulation 1, which is fully polymeric shows the lowest *E* and σ, while showing a considerably high ε. These results are expected, as fully degradable polymers are generally more ductile, but weaker than composite materials (40). The results obtained with formulations 2 and 4 are also in accordance to the literature, as the increase in BGNPs content results in an increase in *E* and σ, but a significant decrease in ε (40). However, the results obtained with formulation 3 were not expected. Although they show the lowest ε registered, as expected from the membranes with the highest BGNPs content, they seem to be less stiff than membranes with formulation 2, and seem to be the membranes that endure the lowest tensions before breaking. It is possible that the quantity of BGNPs present in formulation 3 is too high, and instead of enhancing the overall structure of the nanocomposite, it ends disrupting the structure, leading to a premature failure. These results seem to indicate that, in order to produce membranes with the best overall mechanical performance, it is necessary to optimize the overall BGNPs quantity. One possible solution for this problem can pass by lowering the number of BGNPs deposition steps during the formation of the LbL membranes.

The adhesive properties of the membranes were also studied, as previous studies have shown that LbL coatings produced with the same materials presented an enhanced

adhesive behaviour due to the presence of the catechol groups (21, 22). Figure 8 shows the obtained results.

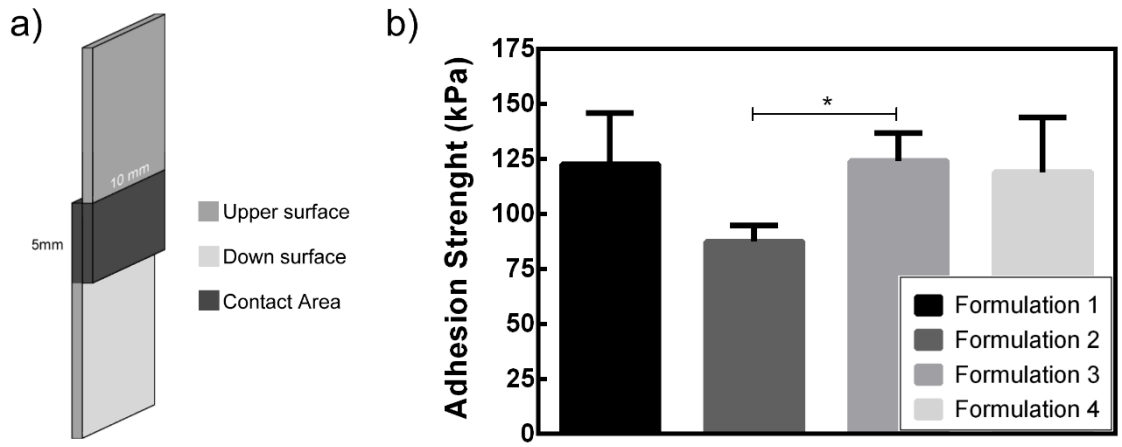

Figure 8 – a) Schematic for the preparation of the membranes for the adhesive strength tests; b) Adhesive strength of the produced membranes. Data are means + standard deviation (n = 3, * significantly different [t-Student test, $p<0.05$]).

As it is observed, only formulation 2 has shown a decrease in its adhesive strength. This may be due to the fact that its end layer is composed of BGNPs and not of HA as in formulations 1 and 4. This behaviour is not observed for the membranes with formulation 3, which also possess and end layer composed of BGNPs. However, formulation 3 is composed with MAPs-inspired HAD conjugate containing catechol groups, which are responsible for the strong bound between mussels and many different surfaces, even in harsh environments (23-25). These catechol groups may explain the significant increase in adhesive strength present in formulation 3, when compared to formulation 2. However, the adhesive behaviour of formulation is comparable to that for formulations 1 and 4. These may be due the presence of BGNPs in the end layer of formulation 3, as they are shown to decrease the adhesive strength when present in the end layer (22). While GTR research is not deeply focusing in enhancing the adhesive properties of GTR membranes, membranes with enhanced adhesion may have a positive effect in this periodontal treatment, as their adhesive nature could help the implantation the membrane *in situ*. The presence of catechol groups has also a positive effect in cell attachment and proliferation (21, 22), which can help with the regeneration of the alveolar bone. As a future work, membranes ending in HAD conjugate should be produced, to confirm if the presence of catechol groups in the end layer of freestanding membranes are able to significantly increase their adhesive properties.

3.7 In vitro bioactivity tests

In vitro bioactivity tests were performed to investigate the apatite formation onto the films under physiological-like conditions. Figure 9 represents the obtained SEM images obtained of the down surface of the produced membranes after immersion in SBF for 7 days at 37 °C.

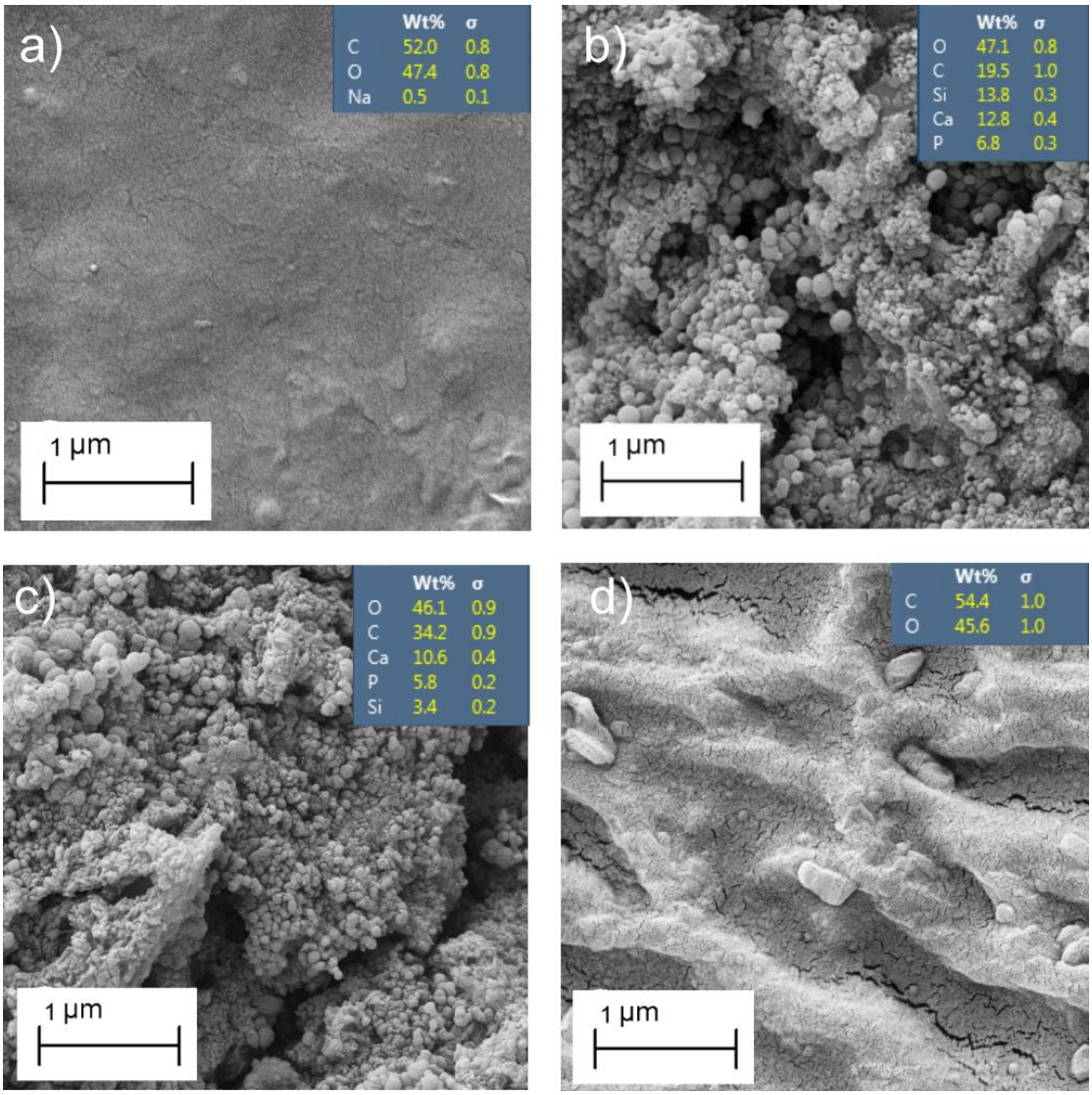

Figure 9 – SEM images and EDS elemental analysis of the freestanding membranes after immersion in SBF at 37 °C for 7 days: a) formulation 1; b) formulation 2; c) formulation 3; d) formulation 4.

After 7 days, only formulations 2 and 3 were able to induce the formation of apatite onto their surface. This is evidenced by the cauliflower-like structures visible in Figures 8 b) and 8 c), which are not visible in formulations 1 and 4, and by the presence of Ca and P peaks in the EDS analysis. Both these results are in accordance to previous works (22, 41). In all formulations it is also possible to detect C and O peaks, which are resulting from the CHI, HA and HAD layers.

The FTIR spectra of the membranes before and after immersion in SBF for 7 days are shown in Figure 10. Again, these images not only show the presence of the

silicate absorption bands (1085 cm^{-1} (asymmetric stretching mode), 800 cm^{-1} (symmetric stretching vibration), and 464 cm^{-1} (rocking vibration of Si−O−S)) in formulations 2 and 3 before immersion in SBF, but after 7 days, it is possible to observe the characteristic bands for carbonated apatite (P−O bending vibration due to the crystalline calcium phosphate phase (600 to 550 cm^{-1}), the band of acidic phosphate group, HPO4 2− (874 cm^{-1}), the peaks assigned to the Ca presence associated with Si−O−Ca bonds (950 cm^{-1}), and the bands representative of the stretching mode of PO4−3 group (1045−1200 cm^{-1})) (22). While the silicate bands are visible in formulation 4 before immersion in SBF, these bands disappear from these membranes after 7 days in SBF. Moreover, there is no sign of carbonated apatite in both formulation 1 and 4. All these results allied indicate that only formulations 2 and 3 are indeed capable of forming an apatite layer onto its surface, which is necessary for proper bone regeneration (26, 27) and, therefore for the envisaged application.

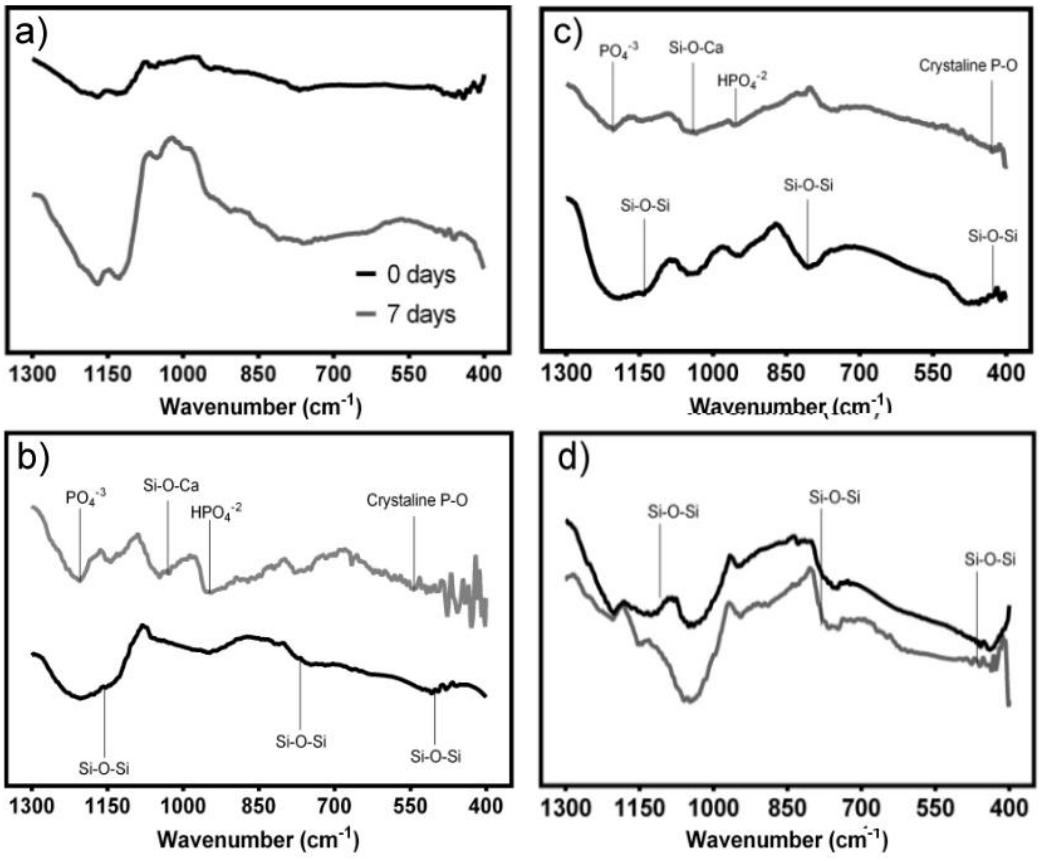

Figure 10 – FTIR spectra of the freestanding membranes before and after immersion in SBF at 37 °C for 7 days: a) formulation 1; b) formulation 2; c) formulation 3; d) formulation 4.

Formulation 4 does not show visible signs of bioactivity and seem to lose its FTIR silicate bands that correlate with the presence of BGNPs. However, the BGNPs concentration in this formulation is significantly lower than in formulations 2 and 3 (Figure 2). As such, the disappearance of the FTIR silicate bands can be due to the

release of most of its BGNPs content. Moreover, the fact that these membranes only possess BGNPs in their interior may difficult the formation of apatite in only 7 days. In fact, WL results may suggest that, for formulation 4, BGNPs are exposed to the environment only after 14 days; therefore, it may be necessary to let these membranes immersed in SBF for a longer time period to induce apatite formation. As future work, the production of membranes with a lower BGNPs quantity present on their surface and not in their interior could be studied, to see if it is the location of the BGNPs that prevents the formation of apatite in formulation 4, or if it is the lower BGNPs concentration present in these membranes that does promote apatite precipitation.

4. CONCLUSIONS

It was possible to produce nacre-inspired freestanding membranes produced by LbL deposition combining CHI, HA and BGNPs. The produced membranes are shown to have different surface properties and bioactive behaviour depending on the overall membrane composition. Biomimetic membranes containing HAD conjugate, which contains the catechol groups responsible by the strong bond between mussels and several surfaces in marine environment, are also shown to have enhanced adhesive properties when compared to membranes with a similar composition, but produced with unmodified HA. It was also shown that there is a necessity to control the BGNPs content inside the membranes to optimize their mechanical performance and degradation profile, without compromising their bioactivity. Overall, the produced membranes show potential to be used in GTR applications, due to their bioactive behaviour necessary for the formation of new bone, tuneable properties and enhanced adhesion.

5. REFERENCES

1. Pihlstrom BL, Michalowicz BS, Johnson NW. Periodontal diseases. Lancet. 2005;366(9499):1809-20.

2. Savage A, Eaton KA, Moles DR, Needleman I. A systematic review of definitions of periodontitis and methods that have been used to identify this disease. Journal of Clinical Periodontology. 2009;36(6):458-67.

3. Gentile P, Chiono V, Tonda-Turo C, Ferreira AM, Ciardelli G. Polymeric membranes for guided bone regeneration. Biotechnology Journal. 2011;6(10):1187-97.
4. Bottino MC, Thomas V, Schmidt G, Vohra YK, Chu TMG, Kowolik MJ, et al. Recent advances in the development of GTR/GBR membranes for periodontal regeneration-A materials perspective. Dental Materials. 2012;28(7):703-21.
5. Luz GM, Mano JF. Biomimetic design of materials and biomaterials inspired by the structure of nacre. Philosophical Transactions of the Royal Society a-Mathematical Physical and Engineering Sciences. 2009;367(1893):1587-605.
6. Sun JY, Bhushan B. Hierarchical structure and mechanical properties of nacre: a review. Rsc Advances. 2012;2(20):7617-32.
7. Katti KS, Mohanty B, Katti DR. Biomimetic lessons learnt from nacre: INTECH. 2010:193-216.
8. Gunnison KE, Sarikaya M, Liu J, Aksay IA, editors. Structure-mechanical property relationships in a biological ceramic-polymer composite: nacre. MRS Proceedings. 1991: Cambridge Univ Press.
9. Burdick JA, Mauck RL. Biomaterials for tissue engineering applications: a review of the past and future trends: Springer Science & Business Media. 2010:1-5.
10. Wang JF, Cheng QF, Tang ZY. Layered nanocomposites inspired by the structure and mechanical properties of nacre. Chemical Society Reviews. 2012;41(3):1111-29.
11. Tang ZY, Wang Y, Podsiadlo P, Kotov NA. Biomedical applications of layer-by-layer assembly: From biomimetics to tissue engineering. Advanced Materials. 2006;18(24):3203-24.
12. Decher G, Hong J, Schmitt J. Buildup of ultrathin multilayer films by a self-assembly process: III. Consecutively alternating adsorption of anionic and cationic polyelectrolytes on charged surfaces. Thin solid films. 1992;210:831-5.
13. Decher G. Fuzzy nanoassemblies: Toward layered polymeric multicomposites. Science. 1997;277(5330):1232-7.
14. Borges J, Mano JF. Molecular Interactions Driving the Layer-by-Layer Assembly of Multilayers. Chemical Reviews. 2014;114(18):8883-942.
15. Jiang CY, Tsukruk VV. Freestanding nanostructures via layer-by-layer assembly. Advanced Materials. 2006;18(7):829-40.

16. Matsusaki M, Ajiro H, Kida T, Serizawa T, Akashi M. Layer-by-Layer Assembly Through Weak Interactions and Their Biomedical Applications. Advanced Materials. 2012;24(4):454-74.
17. Larkin AL, Davis RM, Rajagopalan P. Biocompatible, Detachable, and Free-Standing Polyelectrolyte Multilayer Films. Biomacromolecules. 2010;11(10):2788-96.
18. Caridade SG, Monge C, Gilde F, Boudou T, Mano JF, Picart C. Free-Standing Polyelectrolyte Membranes Made of Chitosan and Alginate. Biomacromolecules. 2013;14(5):1653-60.
19. Gil S, Silva JM, Mano JF. Magnetically Multilayer Polysaccharide Membranes for Biomedical Applications. ACS Biomaterials Science & Engineering. 2015;1(10):1016-25.
20. Croll TI, O'Connor AJ, Stevens GW, Cooper-White JJ. A blank slate? Layer-by-layer deposition of hyaluronic acid and chitosan onto various surfaces. Biomacromolecules. 2006;7(5):1610-22.
21. Neto AI, Cibrao AC, Correia CR, Carvalho RR, Luz GM, Ferrer GG, et al. Nanostructured Polymeric Coatings Based on Chitosan and Dopamine-Modified Hyaluronic Acid for Biomedical Applications. Small. 2014;10(12):2459-69.
22. Rego SJ, Vale AC, Luz GM, Mano JF, Alves NM. Adhesive Bioactive Coatings Inspired by Sea Life. Langmuir. 2016;32(2):560-8.
23. Lee Y, Chung HJ, Yeo S, Ahn C-H, Lee H, Messersmith PB, et al. Thermo-sensitive, injectable, and tissue adhesive sol-gel transition hyaluronic acid/pluronic composite hydrogels prepared from bio-inspired catechol-thiol reaction. Soft Matter. 2010;6(5):977-83.
24. Wilker JJ. Marine bioinorganic materials: mussels pumping iron. Current Opinion in Chemical Biology. 2010;14(2):276-83.
25. Yu ME, Deming TJ. Synthetic polypeptide mimics of marine adhesives. Macromolecules. 1998;31(15):4739-45.
26. Luz GM, Mano JF. Preparation and characterization of bioactive glass nanoparticles prepared by sol-gel for biomedical applications. Nanotechnology. 2011;22(49):11.
27. Luz GM, Mano JF. Nanoengineering of bioactive glasses: hollow and dense nanospheres. Journal of Nanoparticle Research. 2013;15(2):11.
28. Kokubo T, Takadama H. How useful is SBF in predicting in vivo bone bioactivity? Biomaterials. 2006;27(15):2907-15.

29. Cardoso MJ, Caridade SG, Costa RR, Mano JF. Enzymatic Degradation of Polysaccharide-Based Layer-by-Layer Structures. Biomacromolecules. 2016: *in press*.

30. Jameela SR, Jayakrishnan A. Glutaraldehyde cross-linked chitosan microspheres as a long-acting biodegradable drug-delivery vehicle - studies on the in-vitro release of mitoxantrone and in-vivo degradation of microspheres in rat muscle. Biomaterials. 1995;16(10):769-75.

31. Gabbott P. Principles and applications of thermal analysis: John Wiley & Sons. 2008:90.

32. Yu ME, Hwang JY, Deming TJ. Role of L-3,4-dihydroxyphenylalanine in mussel adhesive proteins. Journal of the American Chemical Society. 1999;121(24):5825-6.

33. Lee H, Scherer NF, Messersmith PB. Single-molecule mechanics of mussel adhesion. Proceedings of the National Academy of Sciences of the United States of America. 2006;103(35):12999-3003.

34. Nicklisch SCT, Waite JH. Mini-review: The role of redox in Dopa-mediated marine adhesion. Biofouling. 2012;28(8):865-77.

35. Giovambattista N, Debenedetti PG, Rossky PJ. Effect of surface polarity on water contact angle and interfacial hydration structure. Journal of Physical Chemistry B. 2007;111(32):9581-7.

36. Li X, Shi JL, Dong XP, Zhang LX, Zeng HY. A mesoporous bioactive glass/polycaprolactone composite scaffold and its bioactivity behavior. Journal of Biomedical Materials Research Part A. 2008;84A(1):84-91.

37. Caridade SG, Merino EG, Alves NM, Bermudez VdZ, Boccaccini AR, Mano JF. Chitosan membranes containing micro or nano-size bioactive glass particles: evolution of biomineralization followed by in situ dynamic mechanical analysis. Journal of the Mechanical Behavior of Biomedical Materials. 2013;20:173-83.

38. Valenzuela LM, Michniak B, Kohn J. Variability of Water Uptake Studies of Biomedical Polymers. Journal of Applied Polymer Science. 2011;121(3):1311-20.

39. Baukh V, Huinink HP, Adan OCG, Erich SJF, van der Ven LGJ. Water-Polymer Interaction during Water Uptake. Macromolecules. 2011;44(12):4863-71.

40. Mota J, Yu N, Caridade SG, Luz GM, Gomes ME, Reis RL, et al. Chitosan/bioactive glass nanoparticle composite membranes for periodontal regeneration. Acta Biomaterialia. 2012;8(11):4173-80.

41. Couto DS, Alves NM, Mano JF. Nanostructured Multilayer Coatings Combining Chitosan with Bioactive Glass Nanoparticles. Journal of Nanoscience and Nanotechnology. 2009;9(3):1741-8.